Eng. Sci., 2021, **13**, 98–105

Engineered Science

DOI: https://dx.doi.org/10.30919/es8d1004

Externally Mechanical Force Induced Unusual Defect in the Second Polymorph of Isoniazid/Fumaric Acid Co-crystal

Partha Pratim Bag*

Abstract

In the case of external mechanical forces and other factors, the crystal morphology of the isoniazid/fumaric acid (INH/FUM) co-crystal during the crystallization process will have an impressive phenomenon. Among the two observed polymorphic crystals, namely block shape (Form I) and needle shape (Form II), the second one shows defect by occupying curve morphology. Moreover, the curve crystals show different thermal properties for its original form. This phenomenon suggests the way of defect formation in organic crystal without adding any additives.

Keywords: Co-Crystal, Polymorph; Deformation; Single Crystal; Crystal Packing.
Received: 08 January 2021; Accepted: 24 January 2021.
Article type: Research article.

1. Introduction

It is considered that a single crystal of sharp and straight edges consisting of a continuous crystal lattice through the entire sample without grain boundaries. Moreover, growth of nanocrystal arrested by surfactant produce unusual shaped crystals such as kinetic products.[1-5] Single crystal of diarylethene,[6-9] anthracene derivatives,[10] azobenzene derivatives,[11] salicylideneaniline,[12] olefin-based organic molecules[13] are also be deformed by light induced twisting, bending, curling or changing shape. Recently deformations of several single crystals by applying mechanical force were extensively studied.[14-17] There are number of different types of compounds have been reported to be helically twisted during crystallization. Conversely, it is very rare without any external additive naturally formation of bent or curve single crystals during a slow crystallization process. In recent times a curve single crystal of macrocyclic π-conjugated organic molecule was found due to phase contamination.[18] Indeed, changing the shape of co-crystal during crystallization process could generate defects in crystal. Moreover, formation of defect in organic crystal is very important as it governs the crystal growth, dissolution rate, chemical stability physical stability, bioavailability, hygroscopicity, dehydration, and compaction behaviour.[19]

Isoniazid (INH) and fumaric acid (FUM) in 1:1 molar ratio in 10% methanol-chloroform solution produced two types of suitable single crystals (Fig. 1, image of crystal from optical microscope) and characterized through single-crystal X-ray diffraction, which is reported so far.[20] Our reinvestigation of INH/FUM co-crystals revealed one surprising phenomena, *i.e.*, the curve shape crystals are formed. Interestingly, these crystals appeared when externally mechanical force induced slow evaporation were conducted at different conditions, such as 2-5 °C (cooling), heating at 40 °C, vibration at room temperature and vibration at 2-5 °C. But these special shapes were not obtained from normal slow evaporation. Here, for the first time, we report the formation of the second form of abnormal defects in the INH/FUM co-crystal under the influence of external mechanical forces.[21] We have characterized the defective form by SCXRD, PXRD, SEM, DSC and TGA. In addition, we investigated the interactions theoretically by Crystal Explorer Software.

2. Instrumental method

2.1 Materials and Methods

The following materials and methods are used for this study.

2.1.1. Materials

Isoniazid drug and fumaric acid were purchased from Sigma-Aldrich. Commercially available solvents were used as received without further purification.

Department of Chemistry, SRM University Sikkim, Sikkim 737102, India.

* *Email:* parthap.bag82@yahoo.com (P.P. Bag)

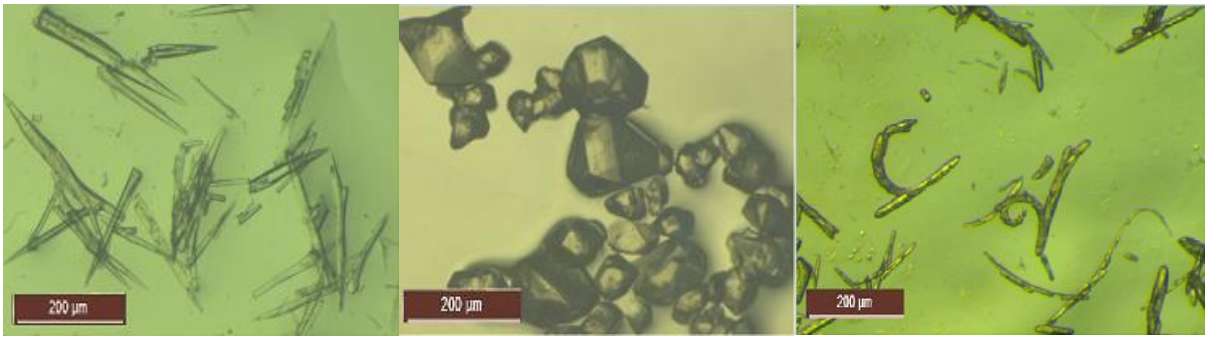

(a) **(b)** **(c)**

Fig. 1 Polymorphs of INH/FUM (a) Form I (Needle), (b) form II (Block) and (c) Form III (Curve).

2.1.2. Methods

Single Crystal Preparation

INH and FUM in 1:1 stoichiometric ratio was subjected to grind in an agate mortar and pestle for 10 min. After grinding, the mixture was transferred to a 10 mL conical flask followed by addition of 10% methanol/chloroform mixture. The suspension was heated at 60 °C until a clear solution was obtained. The resulting mixture was boiled for 10 min followed by filtered into a fresh conical flask. The filtrate was left to evaporate slowly at ambient conditions. The single crystals suitable for X-ray diffraction studies were obtained in 4–6 days.

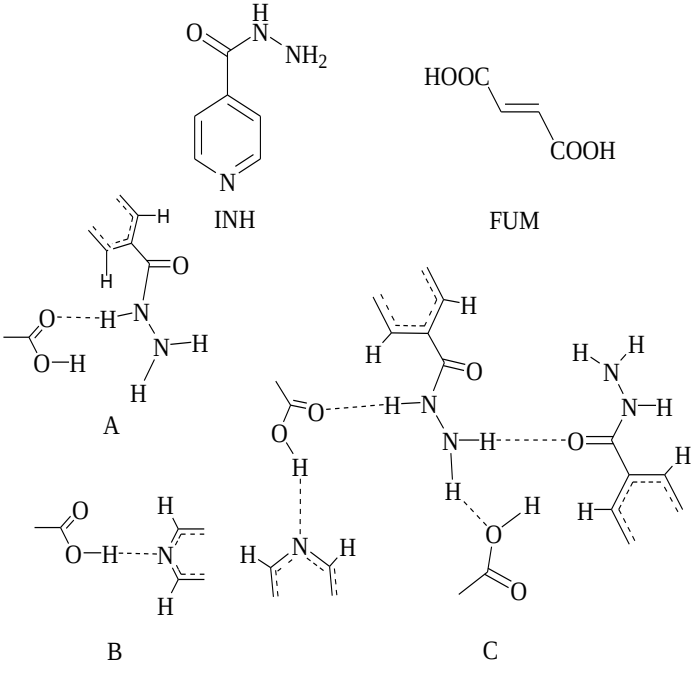

Scheme 1 Supramolecular homo- and heterosynthons exhibited by INH/FUM (1:1) co-crystal polymorphs.

Image of co-crystal at optical microscope

Curve shaped single crystals were prepared in same way with externally mechanical force directed slow evaporation, like 2-5 °C (cooling), heating at 40 °C, vibration at room temperature and vibration at 2-5 °C.

Crystallography Co-crystal of Isoniazid was individually mounted on a glass pip. Intensity data was collected on a Brukar's KAPPA APEX II CCD Duo system with graphite-monochromatic Mo Kα radiation (λ = 0.71073 Å). The data was collected at 296 K (23 °C) temperature. Data reduction was performed using Bruker SAINT software.[22a] Crystal structures were solved by direct methods using SHELXL-97 and refined by full-matrix least-squares on F2 with anisotropic displacement parameters for non-H atoms using SHELXL-97.[22b] Hydrogen atoms associated with carbon atoms were fixed in geometrically constrained positions. Hydrogen atoms associated with oxygen and nitrogen atoms were included in the located positions. Structure graphics shown in the figures were created using the Mercury software.

Powder X-Ray Diffraction (PXRD) The PXRD patterns were collected on a Rigaku SmartLab with a Cu *Kα* radiation (1.540 Å). The tube voltage and amperage were set at 40 kV and 50 mA respectively. Each sample was scanned between 10 and 90° 2θ with a step size of 0.02°/sec. The instrument was previously calibrated using a silicon standard.

Differential Scanning Calorimetry (DSC) DSC was conducted on a Mettler-Toledo DSI1 STAR^e instrument. Accurately weighed samples (2-3 mg) were placed in hermetically sealed aluminium crucibles (40 µL) and scanned from 30 °C to 300 °C at a heating rate of 5 °C/min under a dry nitrogen atmosphere (flow rate 80 mL/min). The data were managed by STAR^e software.

Thermogravimetric Analysis (TGA) TGA was performed on a Mettler-Toledo TGA/SDTA 851^e instrument. Approximately 10-15 mg of the sample was added to an aluminium crucible and heated from 30 to 500 °C at a rate of 10 °C/min under continuous nitrogen purge.

IR Spectroscopy Fourier transmission infrared spectra of the solids were obtained using a Fourier–transform infrared spectrometer (PerkinElmer 502). KBr samples (2 mg in 20 mg

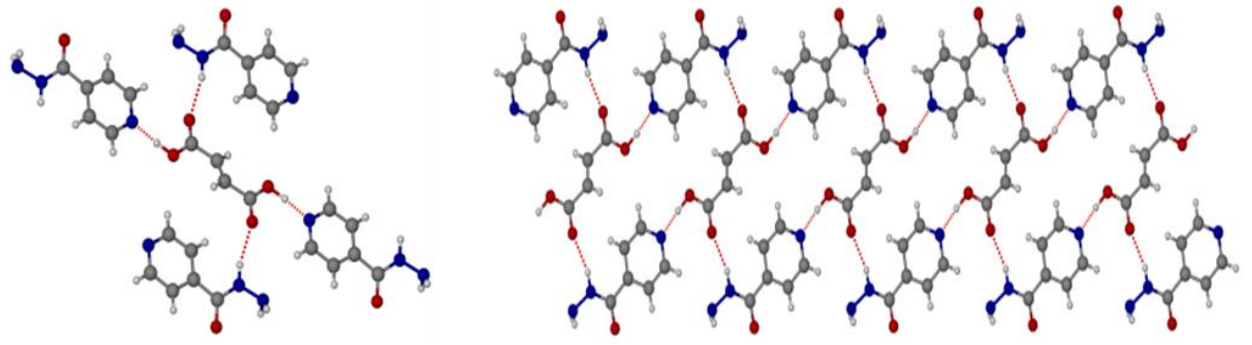

(a) (b)

Fig. 2 Crystal packing in INH/FUM co-crystal polymorph (needle): (a) tetrameric motif, (b) 1D tape forming by terameric synthon. Molecules are colored according to the elements colour. (Color mapping, Blue: N, Red: O, Gray: C and White: H)

of KBr) were prepared and 10 scans were collected at 4 cm^{-1} resolution for each sample. The spectra were measured over the range of 4000-400 cm^{-1}.

Hot Stage Microscopy (HSM) Thermomicroscopic investigations were performed on with an optical polarizing microscope (Leica MZ16) equipped with a Linkam hot-stage. Samples were heated over the temperature range of 30 to 190 °C at a constant heating rate of 2-3 °C min^{-1}.

Scanning Electron Microscopy (SEM) SEM was performed at Cambridge scanning electron microscope with EDAX attachment and JEOL microscope JSM-6700F (Voltage 10 kV, chamber pressure 1.3e^{-4} mbar, magnification x200). For the SEM study, the methanol solutions of were drop casted onto microscopic glass slides, dried and coated with platinum.

Optical Microscopy. The crystal images were taken by using Leica M80 microscope.

3. Results and discussion

The INH molecule has a pyridyl N-atom, one terminal primary amine group (–NH_2) and a secondary amine group (>NH) which is in between the carbonyl group (>C=O) and the terminal primary amine group (–NH_2). The pyridyl N-atom acts as hydrogen bond acceptor and remaining two amine groups (terminal primary amine group (–NH_2) and a secondary amine group (>NH)) act as hydrogen bond donor. But interestingly this terminal primary amine group (–NH_2) did not take part any bond formation in the layer. The conformer, FUM molecule, possesses two strong hydrogen bonding functional groups; two carboxylic hydroxyl groups at the two ends of ethylene moiety and are present as a trans position with respect to carboxylic hydroxyl group and two carboxylic carbonyl O-atom making the presence of inversion symmetry in itself. The two carboxylic hydroxyl groups act as hydrogen bond donor and two carboxylic carbonyl O-atom

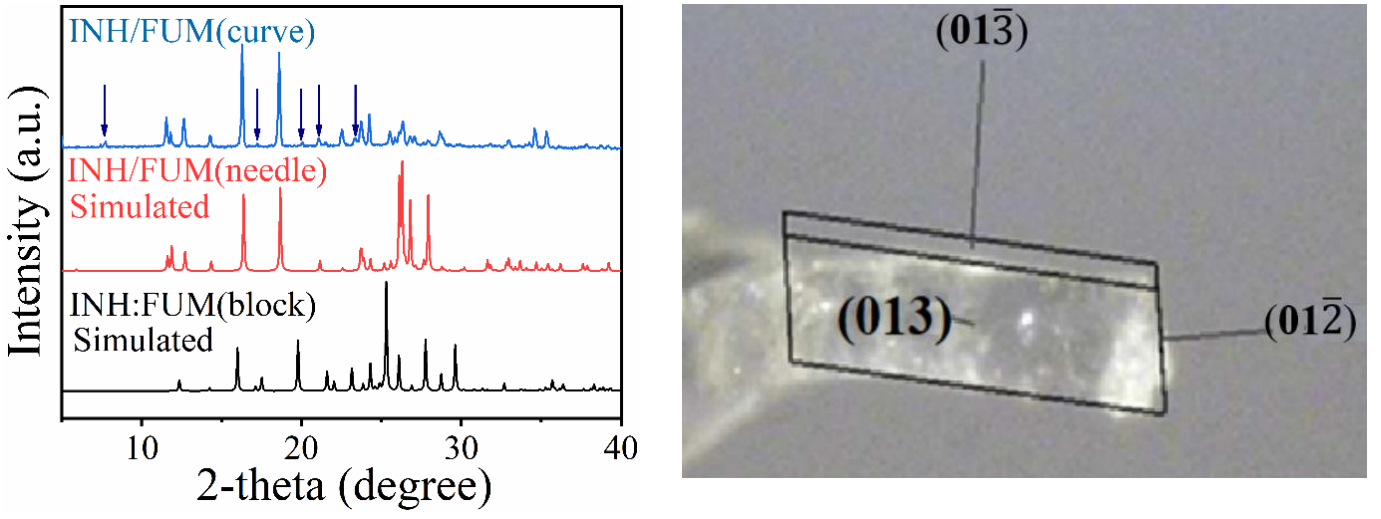

(a) (b)

Fig. 3 (a) PXRD pattern of two polymorphs and curve shaped INH/FUM co-crystal. The arrow indicates the difference between curve and needle co-crystal. (b) Image of the face indexing of curve co-crystal (defective form II), where it shows the (01$\bar{3}$) face is the bending face and the crystal is grown through (10$\bar{2}$) face.

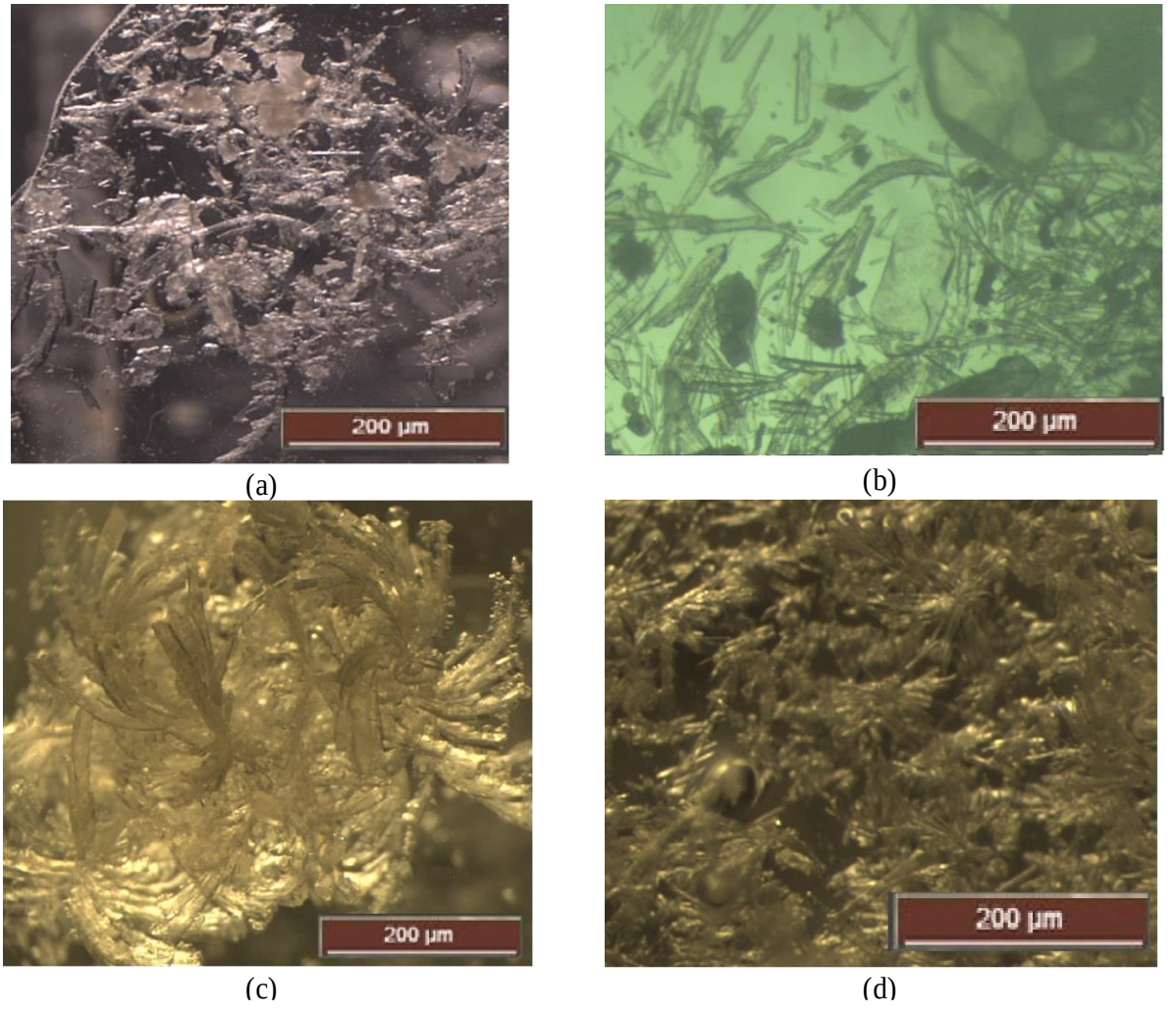

Fig. 4 Optical microscope image (200 µM) of crystals at different condition like (a) Cooling (~ 2-5 °C), (b) Heating (~40 °C), (c) Vibration and (d) Vibration and cooling (~ 2-5 °C).

acts as hydrogen bond acceptor. Hence, in this case the secondary amine group (>N2–H2A) donate hydrogen to carboxylic carbonyl O-atom (>C7=O3) to form a strong N2–H2A…O3; d/Å, θ/°; 2.013 Å, 163.56° *via* synthon A and carboxylic hydroxyl group (O2–H2B) donate hydrogen to pyridyl N-atom (N1) to form a strong O2–H2B…N1; d/Å, θ/°; 1.555 Å, 174.70° *via* synthon B. Both the synthon A and B together reveals a 1D tape (Fig. 2b) where, INH and FUM are alternatively bonded form a tetrameric motif (Fig. 2a). Except these strong interactions, there are few weak interactions like C1–H1…O2; d/Å, θ/°; 2.711 Å, 166.07°; C2–H2…O3; d/Å, θ/°; 2.576 Å, 147.60°; C5–H5…N3; d/Å, θ/°; 2.708 Å, 150.85°.

At PXRD (Fig. 3) the two forms of INH/FUM co-crystals *i,e.*, needle and block are completely different from each other but the curve form is closely similar to the needle form except few new peaks are indicated by arrows. The new peaks are possibly due to dislocation the lattice points, arose from curve shape of crystal. Generally, the defects in crystal like dislocations, epitaxial growth and grain boundaries will introduce a branched growth of crystals with sharp bending. [23-24]

Generally normal crystallization process offers the formation of slow crystal nucleation by following Ostwald dilution law.[25] Slow nucleation favours the formation of non-defective solids by occupying periodic and regular lattice position of molecule in crystal structure. Whereas, external disturbance opposes some extent to form this regular arrangement, which may produce defect in crystals. To obtain a well organize smooth curve shape crystal at the macroscopic level needs distortions at the molecular level.[26] The curve shape of INH/FUM crystal could be achieved by the external mechanical disturbance such as heating, cooling or vibration; possibly encourage the distortion at $(01\ \bar{3})$ face which originates the defect in crystal reveals curve shape (Fig. 3b). Optical microscope images of crystal at different conditions are given in Fig. 4 which shows concomitant formation of two polymorphs along with curve shaped crystals.

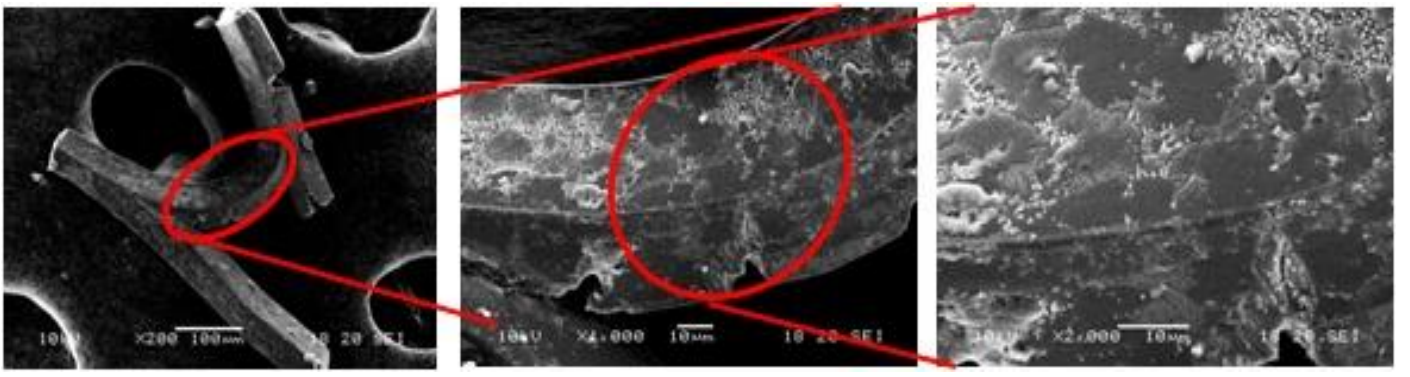

Fig. 5 SEM image of curve INH/FUM co-crystal. Notice at the bent portion there is no junction *i,e.*, it is not twisted crystal.

Although PXRD shows the close similarity between curve shaped and needle form, SEM image (Fig. 5) clarify that it is not a twin crystal, *i.e.*, curve shape of needle crystals is not intergrowth together at different orientation. The extra peaks in PXRD patterns of curve co-crystal are due to defect formation in the needle form by slight changing of lattice points and planes. Several attempts were taken to know the single crystal structure of curve crystal, but due to tiny nature we could not get required diffraction spot for further collect the data. The diffraction spots are showing in Fig. 6.

Thermal property of needle and curve shaped INH/FUM co-crystal DSC and TGA experiment were conducted. DSC gives melting endotherms for INH/FUM (needle) at 172.12 °C along with a pre-melting endotherm at 63.17 °C (Fig. 7) which may be due to phase transition, for curve co-crystal the melting endotherm observed at 169.07 °C with a small melting peak at 83.47 °C. this small melting peak was analysed by Hot Stage Microscopy (HSM) (Fig. 7c and 7d) experiments provide conclusive evidence. The similar pattern of TGA is indicating the similarity between them.

The Hirshfeld surfaces and the associated 2D fingerprint plots were calculated by using the Crystal Explorer[27] program, which accepts a structure input file in the CIF format. A Hirshfeld surface is the outer contour of the space which a molecule or an atom consumes in a crystalline environment. The normalized contact distance d_{norm} based on both d_e (distance from the point to the nearest nucleus external to the surface) and d_i (distance to the nearest nucleus internal to the surface) and the van der Waals (vdW) radii of the atom, given by equation (1), enables identification of the regions of particular importance to intermolecular interactions:

$$d_{norm} = \frac{(d_i - r_i^{vdw})}{r_i^{vdw}} + \frac{(d_e - r_e^{vdw})}{r_e} \quad \text{.....} \quad (1)$$

The value of the d_{norm} is negative or positive when intermolecular contacts are, respectively, shorter or longer than vdW separations. Because of the symmetry between d_e and d_i in the expression for d_{norm}, where two Hirshfeld surfaces touch, both will display a red spot with the same identical as well as size and shape. The d_{norm} values are mapped onto the Hirshfeld surface using a red–blue–white colour scheme: red regions correspond to closer contacts and negative d_{norm} value, the blue regions correspond to longer contacts and positive d_{norm} value and the white regions are those where the distance of contacts is exactly the vdW separation and with a d_{norm} value of zero. The

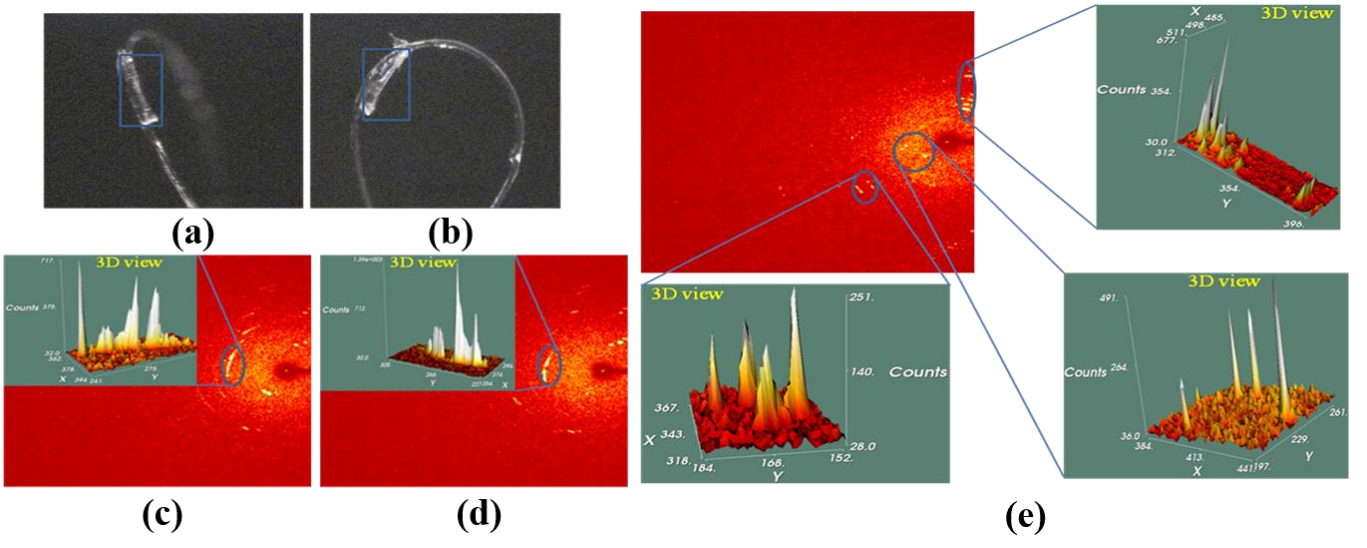

Fig. 6 (a and b) Image of the mounting crystal, (c-e) X-ray diffraction spot at SCXRD at X-ray exposed time 30 sec/image using Cu source (λ=1.54051).

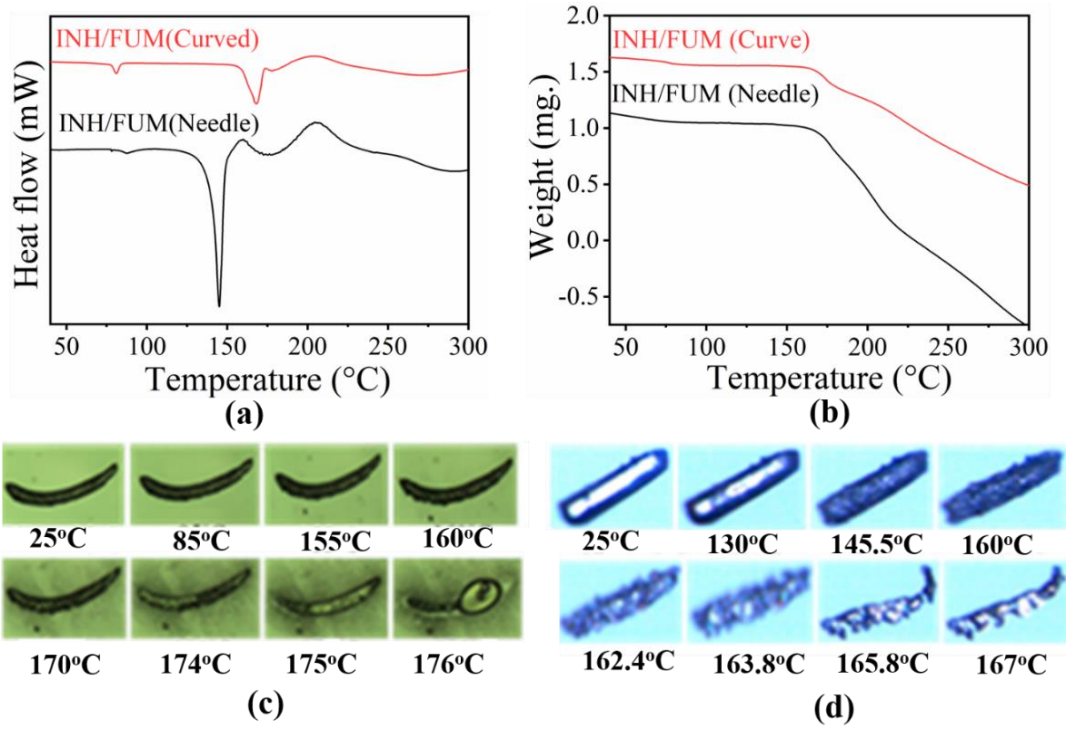

Fig. 7 (a) DSC, (b) TGA, (c) and (d) HSM of curve and needle co-crystal of INH/FUM.

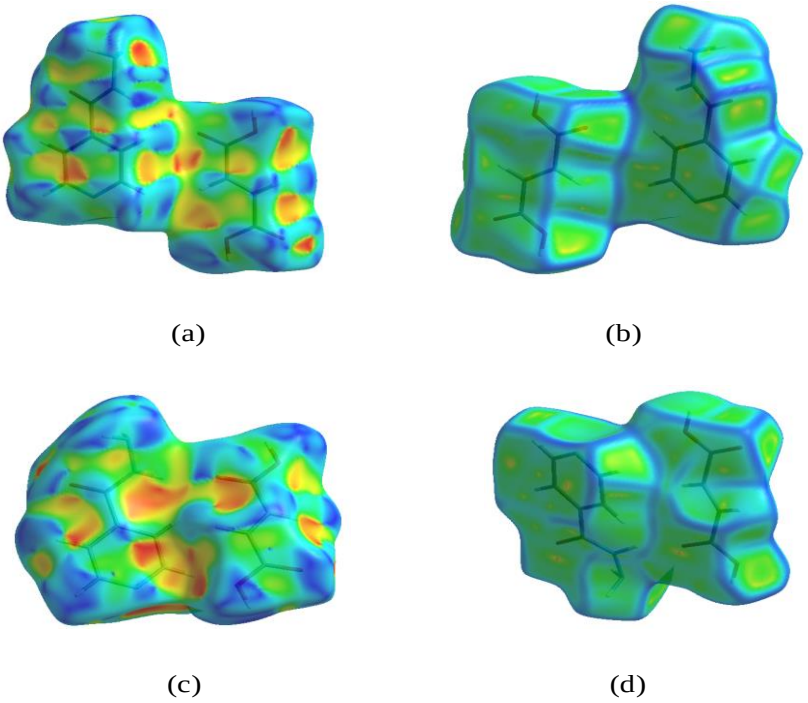

Fig. 8 (a) Hirshfeld surface (surface index), (b) Hirshfeld surface (curveness) of INH/FUM (needle) polymorph-I and (c) Hirshfeld surface (surface index), (d) Hirshfeld surface (curveness) of INH/FUM (block) polymorph-II.

combination of *d*e and *d*i in the form of a 2D fingerprint plot provides summary of intermolecular contacts in the crystal. The respective acceptor and donor atoms showing strong C-H···N intermolecular hydrogen bonds are indicated as bright red spots on the Hirshfeld surface (Fig. 8a and 8c). This finding is substantiated by the calculated electrostatic potential (Fig. 8b and 8d) of the molecule that was used to generate the Hirshfeld surface. The negative potential (acceptor) is indicated as a red surface around the two nitrogen atoms and the blue surface area, indicating the positive potential (donor), is mapped in the proximity of the hydrogen atoms.

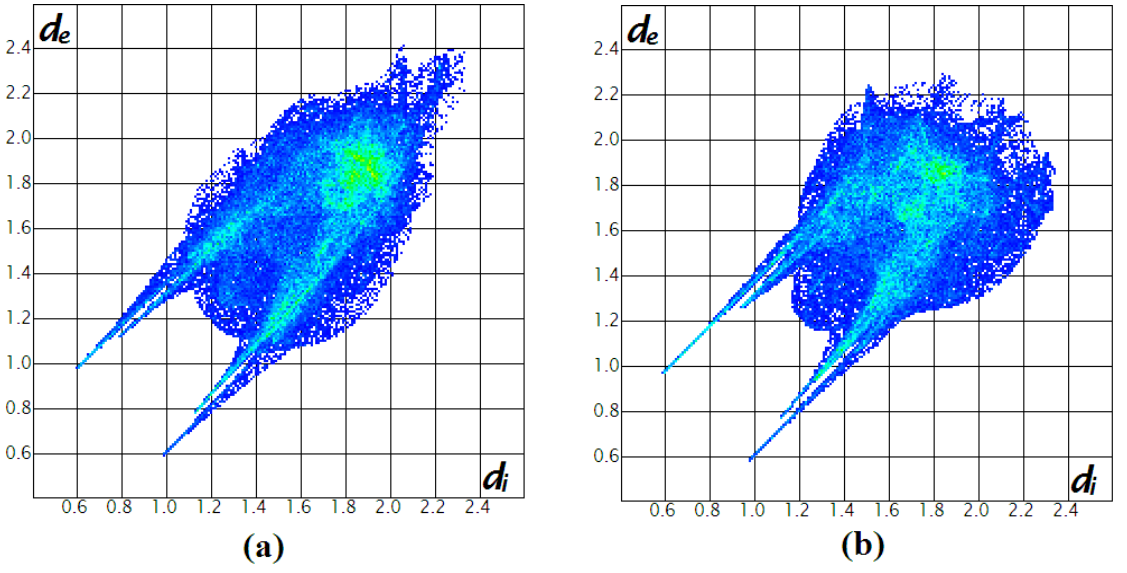

Fig. 9 Fingerprint plot of (a) INH/FUM (Needle) form I, (b) INH/FUM (Block) form II.

The two polymorphs those structures we already got, easily distinguished with the help of Hirshfeld surface analysis. To generate the Hirshfeld surface we used the surface resolution standard (high). Here we took the two picture namely surface index and curveness (Fig. 8). The fingerprint plot of two polymorphs of INH/FUM co-crystal is showing a clear distinction between them. The shape of Hirshfeld surface analysis is different which also approved this result (Fig. 9).

4. Conclusion

In conclusion, we noticed for the first time that defective crystal (here, curve shaped crystal) can be achieved by simple external mechanical force like heating, cooling or vibration which encourage the defect formation at $(01\bar{3})$ face which originates the defect in crystal reveals curve shape. The defects are created due to disturbance of crystal nucleation which changes the position of lattice point and planes. This is the beauty of crystal engineering.[28] The technique provides an efficient procedure to produce defect without adding any additives. We are currently undertaking the single crystal growth by employing various methods to determine their crystal structures.

Acknowledgement

PPB gratefully acknowledged Prof. C. Malla Reddy from IISER Kolkata for providing experimental facility and thanks the Seed Grant for research and Collaborative Research Funds under TEQIP III.

Supporting Information

Not applicable

Conflict of Interest

There are no conflicts to declare.

References

[1] H. C. Camargo, Y. J. Xiong, L. Ji, J. M. Zuo, Y. N. Xia, *J. Am. Chem. Soc.*, 2007, **129**, 15452, doi: 10.1021/ja077505a.

[2] W. Han, L. Yi, N. Zhao, A. Tang, M. Gao, Z. Tang, *J. Am. Chem. Soc.*, 2008, **130**, 13152, doi: 10.1021/ja8046393.

[3] X. Li, J. Z. Niu, H. Shen, W. Xu, H. Wang, L. S. Li, *Cryst. Eng. Comm.*, 2010, **12**, 4410, doi: 10.1039/C0CE00025F.

[4] L. Tian, M. T. Ng, N. Venkatram, W. Ji, J. J. Vittal, *Cryst. Growth Des.*, 2010, **10**, 1237, doi: 10.1021/cg901254j.

[5] T. Yu, J. Joo, Y. II. Park, T. Hyeon, *Angew. Chem. Int. Ed.*, 2005, **44**, 7411, doi: 10.1002/anie.200500992.

[6] D. Kitagawa, H. Nishi, S. Kobatake, *Angew. Chem. Int. Ed.*, 2013, **52**, 9320, doi: 10.1002/anie.201304670.

[7] F. Terao, M. Morimoto, M. Irie, *Angew. Chem. Int. Ed.*, 2012, **51**, 901, doi: 10.1002/anie.201105585.

[8] L. Kuroki, S. Takami, K. Yoza, M. Morimoto, M. Irie, *Photochem. Photobiol. Sci.*, 2010, **9**, 221, doi: 10.1039/B9PP00093C.

[9] M. Irie, S. Kobatake, M. Horichi, *Science*, 2001, **291**, 1769, doi: 10.1126/science.291.5509.1769.

[10] L. Zhu, R. O. Al-Kaysi, C. J. Bardeen, *J. Am. Chem. Soc.*, 2011, **133**, 12569, doi: 10.1021/ja201925p.

[11] O. S. Bushuyev, T. A. Singleton, C. J. Barrett, *Adv. Mater.*, 2013, **25**, 1796, doi: 10.1002/adma.201204831.

[12] H. Koshima, K. Takechi, H. Uchimoto, M. Shiro, D. Hashizume, *Chem. Commun.*, 2011, **47**, 11423, doi: 10.1039/C1CC14288G.

[13] J.-K. Sun, W. Li, C. Chen, C.-X. Ren, D.-M. Pan, J. Zhang, *Angew. Chem. Int. Ed.*, 2013, **52**, 6653, doi: 10.1002/anie.201301207.

[14] S. Ghosh, C. M. Reddy, *Angew. Chem. Int. Ed.*, 2012, **51**, 10319, doi: 10.1002/anie.201204604.
[15] S. Ghosh, M. K. Mishra, S. B. Kadambi, U. Ramamurty, G. R. Desiraju, *Angew. Chem. Int. Ed.*, 2015, **54**, 2674, doi: 10.1002/anie.201410730.
[17] M. K. Panda, S. Ghosh, N. Yasuda, T. Moriwaki, G. D. Mukherjee, C. M. Reddy, P. Naumov, *Nat. Chem.*, 2015, **7**, 65, doi: 10.1038/nchem.2123.
[18] L. Zhang, P. Naumov, *Angew. Chem. Int. Ed.*, 2015, **54**, 8642, doi: 10.1002/anie.201504153.
[19] C.-M. Chou, S. Nobusue, S. Saito, D. Inoue, D. Hashizume, S. Yamaguchi, *Chem. Sci.*, 2015, **6**, 2354, doi: 10.1039/C4SC03849E.
[20] (a) M. D. Eddleston & W. Jones, Disordered Pharmaceutical Materials, 2016, 103. (b) P. P. Bag, G. P. Singh, S. Singha, G. Roymahapatra, *Eng. Sci.*, 2021, **13**, 1, doi: 10.30919/es8d1166. (c) Y. Fu, P. Zhao, L. Yang, R. Miao, C. Zhang, Z. Guo, Y. Liu, *ES Mater. Manufact.*, 2018, **1**, 50, doi: 10.30919/esmm5f126.
[21] S. Cherukuvada, A. Nangia, *Cryst. Eng. Comm.*, 2012, **14**, 2579, doi: 10.1039/C2CE06391C.
[22] G. R. Desiraju, *Angew. Chem. Int. Ed. Engl.*, 1995, **34**, 2311, doi: 10.1002/anie.199523111.
[23] (a) SAINT Plus (version 6.45); Bruker AXS Inc.: Madison, WI, 2003. (b) SMART (version 5.625) and SHELX-TL (version 6.12); Bruker AXS Inc.: Madison, WI, 2000.
[24] K.-W. Benz, W. Neumann, Introduction to Crystal Growth and Characterization, 1st ed., Ch. 4, 2014, pp. 301–413. Weiheim: Wiley-VCH Verlag, doi: 10.1002/9783527689248.
[25] A. A. Chernov, Modern Crystallography, Vol. III. Crystal Growth. Berlin: Springer Verlag, 1984, doi: 10.1007/978-3-642-81835-6.
[26] W. eiZ. Ostwald, *Phys. Chem.*, 1879, **22**, 289.
[27] S. K. Wolff, D. J. Grimwood, J. J. McKinnon, M. J. Turner, D. Jayatilaka, M. A. Spackman, 2013 Crystal Explorer Version 3.1 (Perth: University of Western Australia).
[28] C. E. Mulijanto, H. S. Quah, G. K. Tan, B. Donnadieu, J. J. Vittal, IUCrJ, 2017, **4**, 65, doi: 10.1107/S2052252516019072.

Author information

Partha Pratim Bag *is presently working as Assistant Professor in SRM University Sikkim, Department of Chemistry, Sikkim, India. He obtained his Ph.D. from IISER Kolkata in 2013. Successively, he completed two Postdoctoral Studies from China (2014-2016 and 2016-2018). He was Assistant Professor in Department of basic Science and Humanities (Chemistry), Dumka Engineering College, Jharkhand from 2018-2020. During his 12 years research tenure, he published several top lined journals including research articles, books and book chapters. His research interest is Crystal Engineering, Solid State Chemistry, Chemical Sensor and Supramolecular nanomaterials.*